JB
Journals.ASM.org

Synthesis of Lipoteichoic Acids in *Bacillus anthracis*

Gabriella Garufi,[a,b] Antoni P. Hendrickx,[b] Karen Beeri,[b] Justin W. Kern,[b]* Anshika Sharma,[a] Stefan G. Richter,[a,b] Olaf Schneewind,[a,b] and Dominique Missiakas[a,b]

Howard Taylor Ricketts Laboratory, Argonne National Laboratory, Argonne, Illinois, USA,[a] and Department of Microbiology, University of Chicago, Chicago, Illinois, USA[b]

Lipoteichoic acid (LTA), a glycerol phosphate polymer, is a component of the envelope of Gram-positive bacteria that has hitherto not been identified in *Bacillus anthracis*, the causative agent of anthrax. LTA synthesis in *Staphylococcus aureus* and other microbes is catalyzed by the product of the *ltaS* gene, a membrane protein that polymerizes polyglycerol phosphate from phosphatidyl glycerol. Here we identified four *ltaS* homologues, designated *ltaS1* to *-4*, in the genome of *Bacillus anthracis*. Polyglycerol phosphate-specific monoclonal antibodies were used to detect LTA in the envelope of *B. anthracis* strain Sterne (pXO1$^+$ pXO2$^-$) vegetative forms. *B. anthracis* mutants lacking *ltaS1*, *ltaS2*, *ltaS3*, or *ltaS4* did not display defects in growth or LTA synthesis. In contrast, *B. anthracis* strains lacking both *ltaS1* and *ltaS2* were unable to synthesize LTA and exhibited reduced viability, altered envelope morphology, aberrant separation of vegetative forms, and decreased sporulation efficiency. Expression of *ltaS1* or *ltaS2* alone in *B. anthracis* as well as in other microbes was sufficient for polyglycerol phosphate synthesis. Thus, similar to *S. aureus*, *B. anthracis* employs LtaS enzymes to synthesize LTA, an envelope component that promotes bacterial growth and cell division.

Structural analysis of lipoteichoic acid (LTA) purified from *Staphylococcus aureus*, *Bacillus subtilis*, *Enterococcus faecalis*, and many other species revealed a polymer of glycerol phosphate linked to glycolipid, which provides for LTA anchoring in bacterial membranes (3, 5, 10, 38). Based on data from the *in vivo* and *in vitro* synthesis of LTA from radiolabeled precursors, a model was proposed whereby phosphatidyl glycerol is polymerized to generate the products polyglycerol phosphate and diacylglycerol (8, 11, 14). In agreement with this model, *S. aureus* LtaS, a polytopic membrane protein with an extracellular domain, is both necessary and sufficient for LTA synthesis from phosphatidyl glycerol (17). The expression of *ltaS* in *S. aureus* or *ltaS* homologues in *B. subtilis* and *Listeria monocytogenes* contributes to bacterial growth under physiological conditions (37°C) in the laboratory (17, 22, 34, 40, 42). These findings suggest that LTA synthesis may also be essential for the growth of Gram-positive bacteria during infection and that LTA inhibitors may be useful therapeutics for infectious diseases caused by Gram-positive microbes (17).

To investigate teichoic acids of *Bacillus anthracis*, the causative agent of anthrax disease (27), Molnár and Prágai used acid hydrolysis of bacterial envelope preparations but failed to detect either glycerol or ribitol, the constituents of LTA and wall teichoic acids (WTA), respectively (32). More recent work studied the contribution of the *dltABCD* operon to *B. anthracis* pathogenesis (12). Initially identified by Heaton and Neuhaus, the *dltABCD* operon of *Lactobacillus casei* was demonstrated to encode factors that catalyze the D-alanyl esterification of polyglycerol phosphate LTA as well as polyribitol phosphate WTA (18, 19, 35). An insertional lesion in the *dltABCD* operon of *B. anthracis* strain Sterne (pXO1$^+$ pXO2$^-$) caused the variant to display increased sensitivity to some antibacterial peptides as well as attenuation in a mouse model of respiratory anthrax (9). Unlike the *B. anthracis* Sterne parent, the *dltABCD* variant did not harbor esterified alanine in the cell wall envelope (12). Nevertheless, these studies did not identify the molecular nature of alanine esterification in the envelope of *B. anthracis*.

The secondary cell wall polysaccharide of *B. anthracis* is tethered to the cell wall envelope through murein linkage units (4, 23), a structure that in other Gram-positive bacteria is used for the immobilization of wall teichoic acid (2, 46). Although the genome of *B. anthracis* harbors *tagO* and other genes known to be involved in the synthesis of the cell wall linkage unit (23, 29), this microbe lacks the genes that are known to be required for wall teichoic acid synthesis (37, 45).

To explore the possibility that *B. anthracis* may synthesize LTA, we used in this study a bioinformatic approach and searched the genome of *B. anthracis* for homologues of *S. aureus* LtaS ($LtaS_{SA}$). This search identified four polytopic membrane proteins with a conserved sulfatase (LtaS) domain, which were designated LtaS1, LtaS2, LtaS3, and LtaS4. Genetic analyses revealed that the *ltaS1* and *ltaS2* genes were both necessary and sufficient for LTA synthesis in *B. anthracis* and in other bacterial species. *B. anthracis* variants unable to synthesize LTA displayed multiple defects in envelope assembly that may account for the inability of mutant bacilli to sporulate and to separate dividing cells during their vegetative life cycle. These findings are in agreement with the general concept that LTA is an essential constituent of the envelope of Gram-positive organisms (33).

MATERIALS AND METHODS

Bacterial growth. *B. anthracis* strain Sterne 34F2 and variants were grown in brain heart infusion (BHI), nutrient broth yeast extract (NBY), or Luria-Bertani (LB) medium at 37°C or 30°C when appropriate. *S. aureus* was grown in tryptic soy broth (TSB). *Escherichia coli* was grown in LB medium. Antibiotics were added to cultures as needed (spectinomycin, 200 μg/ml, and kanamycin, 20 to 50 μg/ml). Expression from the tetra-

Received 16 April 2012 Accepted 2 June 2012
Published ahead of print 8 June 2012
Address correspondence to Dominique Missiakas, dmissiak@bsd.uchicago.edu.
* Present address: Justin W. Kern, Department of Developmental Biology, Stanford University, Stanford, California, USA.
Supplemental material for this article may be found at http://jb.asm.org/.

doi:10.1128/JB.00626-12

TABLE 1 Strains and plasmids used in this study

Designation	Genotype	Description	Reference
Bacillus anthracis strains			
WT	WT	*B. anthracis* Sterne 34F2	
ltaS1	Δ*ltaS1*	Sterne with an *ltaS1* gene deletion	This work
	ltaS1::Sp	Sterne with *bursa aurealis* insertion in *ltaS1*	
ltaS2	Δ*ltaS2*	Sterne with an *ltaS2* gene deletion	This work
ltaS3	Δ*ltaS3*	Sterne with an *ltaS3* gene deletion	This work
	ltaS3::Km	Sterne with *bursa aurealis* insertion in *ltaS3*	
ltaS4	*ltaS4*::Spc	Sterne with *bursa aurealis* insertion in *ltaS4*	This work
ltaS1 ltaS2	*ltaS1*::Spc-Δ*ltaS2*	*ltaS1*::Spc allele transduced in Sterne Δ*ltaS2*	This work
ltaS1 ltaS3	*ltaS1*::Sp-*ltaS3*::Km	*ltaS1*::Spc allele transduced in Sterne *ltaS3*::Km	This work
ltaS1 ltaS4	Δ*ltaS1-ltaS4*::Spc	*ltaS4*::Spc allele transduced in Sterne Δ*ltaS1*	This work
ltaS2 ltaS3	Δ*ltaS2-ltaS3*::Km	*ltaS3*::Km allele transduced in Sterne Δ*ltaS2*	This work
ltaS2 ltaS4	Δ*ltaS2-ltaS4*::Sp	*ltaS4*::Sp allele transduced in Sterne Δ*ltaS2*	This work
ltaS3 ltaS4	*ltaS3*::Km-*ltaS4*::Sp	*ltaS4*::Spc allele transduced in Sterne *ltaS3*::Km	This work
ltaS1 ltaS3-4	Δ*ltaS1-ltaS3*::Km-*ltaS4*::Sp	*ltaS4*::Spc and *ltaS3*::Km alleles transduced in Sterne Δ*ltaS1*	This work
Staphylococcus aureus strains			
ANG499 p*itet* with no insert	*spac-ltaS*$_{SA}$ *tet*	*S. aureus* with IPTG (*spac*)-inducible *ltaS*$_{SA}$	17
ANG499 p*itet* with *ltaS*$_{SA}$	*spac-ltaS*$_{SA}$ *tet-ltaS*$_{SA}$	*S. aureus* with both (*spac*) IPTG- and anhydrotetracycline (*tet*)-inducible *ltaS*$_{SA}$	17
ANG499 p*itet* with *ltaS1*	*spac-ltaS*$_{SA}$ *tet-ltaS1*	*S. aureus* with IPTG (*spac*)-inducible *ltaS*$_{SA}$ and anhydrotetracycline (*tet*)-inducible *ltaS1*	This work
Vectors and plasmids			
pJK4	No insert	Empty vector JK4 with no insert	24
p*ltaS1*	*ltaS1*	Plasmid pJK4 carrying *ltaS1* under the control of the IPTG-inducible (*spac*) promoter	This work
p*ltaS2*	*ltaS2*	Plasmid pJK4 carrying *ltaS2* under the control of the IPTG-inducible (*spac*) promoter	This work
p*ltaS3*	*ltaS3*	Plasmid pJK4 carrying *ltaS3* under the control of the IPTG-inducible (*spac*) promoter	This work
p*ltaS4*	*ltaS4*	Plasmid pJK4 carrying *ltaS4* under the control of the IPTG-inducible (*spac*) promoter	This work
pPROEX-s*ltaS1*	Soluble domain of LtaS1 (sLtaS1)	Plasmid used for production of recombinant sLtaS1	This work
pPROEX-s*ltaS2*	Soluble domain of LtaS2 (sLtaS2)	Plasmid used for production of recombinant sLtaS2	This work
pPROEX-s*ltaS3*	Soluble domain of LtaS3 (sLtaS3)	Plasmid used for production of recombinant sLtaS3	This work
pPROEX-s*ltaS4*	Soluble domain of LtaS4 (sLtaS4)	Plasmid used for production of recombinant sLtaS4	This work

cycline-inducible promoter (P_{tet}) was induced by adding 150 ng/ml anhydrotetracycline to the medium, and expression via the *spac* promoter (P_{spac}) was induced by the addition of 1 mM isopropyl-β-D-thiogalactopyranoside (IPTG).

***B. anthracis* strains and plasmids.** The strains and plasmids used in this study are listed in Table 1. The alleles *ltaS1*::Spc, *ltaS3*::Kan, and *ltaS4*::Spc were obtained following transposon mutagenesis of *B. anthracis* Sterne with the *bursa aurealis* minitransposon (41). Transduction using bacteriophage CP-51 was performed for each marked allele using the *B. anthracis* Sterne wild-type or mutant background carrying unmarked mutations in *ltaS* genes (15). Newly transduced alleles were selected by growing bacteria at 30°C on appropriate selective medium and validated by sequencing the DNA of the transposon insertion site using inverse PCR as described previously (41). Unmarked *B. anthracis* variants (Δ*ltaS1*, Δ*ltaS2*, and Δ*ltaS3* mutants) were generated by allelic replacement using plasmid pLM4 as previously described (30). All strains were verified by DNA sequencing and immunoblotting with LtaS-specific antibodies. Mutants carrying insertions or deletions in the *ltaS1* or *ltaS3* gene displayed identical phenotypes, respectively. For simplicity, no distinction was made between these alleles and strains are referred to by the names listed in the "designation" column of Table 1. The *E. coli-B. anthracis* shuttle plasmid pJK4 was used to clone the *ltaS* genes with an IPTG-inducible promoter (24) and was used for both complementation studies and sufficiency experiments using *E. coli* as a host (see below). Primers used to amplify the *ltaS* open reading frames by PCR amplification from genomic DNA are listed in Table 2. Plasmid pPROEX (Invitrogen) was used to express the predicted soluble domains (as depicted in Fig. 1B) of LtaS1, LtaS2, LtaS3, and LtaS4 in *E. coli.* Primers used to amplify the corresponding genomic DNA are listed in Table 2.

Inducible expression of *ltaS1* in *S. aureus*. Primers were used to amplify *ltaS1* from *B. anthracis* and ligated with vector carrying the P_{tet} promoter as described earlier (17). The recombinant plasmid was inserted into the chromosome of *S. aureus* strain ANG499 (17), yielding the *S. aureus* strain with IPTG-inducible *ltaS*$_{SA}$ (P_{spac}-*ltaS*$_{SA}$) and anhydrotetracycline-inducible *ltaS1* (P_{tet}-*ltaS1*). Strains ANG513 (ANG499 P_{tet} with no insert) and ANG514 (ANG499 P_{tet}-*ltaS*$_{SA}$) were used as controls (17). All primer sequences used for this study are listed in Table 2.

Immunoblot analyses. *B. anthracis* cultures were grown in BHI and normalized to an optical density at 600 nm (OD_{600}) of 5. Two milliliters of normalized culture was mixed with 1 ml of 0.1-mm glass beads to disrupt the bacterial envelope with a bead beater (BioSpec Products, Bartlesville, OK) by shearing five times for 2 min at 4°C. Glass beads and cell debris were sedimented by centrifugation at 200 × *g* for 1 min. Two samples of 0.5 ml of supernatant were transferred to two new tubes. One sample was used for analysis of LTA and centrifuged at 16,000 × *g* for 15 min. Sedimented material was suspended in 100 μl of sample buffer with 2% SDS

TABLE 2 Sequences of primers used in this study

Name	Sequence	Use
BAS2737 KO 1Kb UP XmaI F	TTTCCCGGGGTACGACGTTTTCGTGCTAAG	Allelic replacement of *ltaS1*
BAS2737 KO 1Kb UP KpnI R	TTTGGTACCCGGAAGGGGAAGCTAAATAA	Allelic replacement of *ltaS1*
BAS2737 KO 1Kb DN KpnI F	TTTGGTACCATTTCTCCACCTCTTTTGATCAT	Allelic replacement of *ltaS1*
BAS2737 KO 1Kb DN EcoRI R	TTTGAATTCAACTTCTCAATCTTACTTCCCAAGAG	Allelic replacement of *ltaS1*
BAS2737 XbaI F	TTTTCTAGAGGATGATCAAAAGAGGTGGAG	Expression of LtaS1 in *E. coli*
BAS2737 KpnI R	TTTGGTACCTTATTTAGCTTCCCCTTCCG	Expression of LtaS1 in *E. coli*
BAS2737 AvrII F	TTTCCTAGGGGATGATCAAAAGAGGTGGAG	Expression of LtaS1 in *S. aureus*
BAS2737 BamHI R	TTTGGATCCTTATTTAGCTTCCCCTTCCG	Expression of LtaS1 in *S. aureus*
BAS2737 BamHI F	TTTGGATCCGATGGAGATAATATGACGGAAGT	Cloning of sLtaS1
BAS2737 HindIII R	TTTAAGCTTTTATTTAGCTTCCCCTTCCGG	Cloning of sLtaS1
BAS5081 KO 1Kb UP XmaI F	TTTCCCGGGCAACCGGAAGGGATATTAAGTTTA	Allelic replacement of *ltaS2*
BAS5081 KO 1Kb UP KpnI R	TTTGGTACCTTTCATTCATTTCCACCCTTTCTC	Allelic replacement of *ltaS2*
BAS5081 KO 1Kb DN KpnI F	TTTGGTACCGAGTAATCTCAGCCTCTTTTTTTATA	Allelic replacement of *ltaS2*
BAS5081 KO 1Kb DN EcoRI R	TTTGAATTCTGATATCACAGCGTAGCCAG	Allelic replacement of *ltaS2*
BAS5081 XbaI F	TTTTCTAGACGACCAAGCCTGATAGAGAAA	Expression of LtaS2 in *E. coli* and *B. anthracis*
BAS5081 KpnI R	TTTGGTACCTTACTCAGCGCTCTTCTTTTCTT	Expression of LtaS2 in *E. coli* and *B. anthracis*
BAS5081 BamHI F	TCTTGGATCCGACGGTAGTAAGTTACAGGAAAC	Cloning of sLtaS2
BAS5081 HindIII R	GTCCAAGCTTTTACTCAGCGCTCTTCTTTTCTTC	Cloning of sLtaS2
BAS3608 KO 1Kb UP XmaI F	TTTCCCGGGGATTTCACAGCAACTACGTACTGT	Allelic replacement of *ltaS3*
BAS3608 KO 1Kb UP KpnI R	TTTGGTACCTAAATAAAAAGTAAAAATGTGGAAGAAATATGTTAAAT	Allelic replacement of *ltaS3*
BAS3608 KO 1Kb DN KpnI F	TTTGGTACCGAAAAATAATGTAAATATGAAAAGGGAGCAA	Allelic replacement of *ltaS3*
BAS3608 KO 1Kb DN EcoRI R	TTTGAATTCGGATGCTATTAAGTGGAATGAAGATAT	Allelic replacement of *ltaS3*
BAS3608 XbaI F	TTTTCTAGAAAGTTAAATAAATTGTATAAAGAAGGTGTAAAAATG	Expression of LtaS3 in *E. coli*
BAS3608 KpnI R	TTTGGTACCTTATTTTTCAGTTTCTTTAATTTTAGTTTGTACTTC	Expression of LtaS3 in *E. coli*
BAS3608 BamHI F	TCTTGGATCCGATAGTAGCAAATTACAAGAAACAGAAAA	Cloning of sLtaS3
BAS3608 HindIII R	GTCCAAGCTTTTATTTTTCAGTTTCTTTAATTTTAGTTTGTACTTC	Cloning of sLtaS3
BAS1327 XbaI F	TTTTCTAGAGAACTGTCATGCTTTTTAGGAGAG	Expression of LtaS4 in *E. coli*
BAS1327 KpnI R	TTTGGTACCCTATTCAAATTTCGTTGTCATCG	Expression of LtaS4 in *E. coli*
BAS1327 BamHI F	TTTGGATCCAGTGGGGACGGGTTCTCTG	Cloning of sLtaS4
BAS1327 HindIII R	TTTAAGCTTCTATTCAAATTTCGTTGTCATCGTTC	Cloning of sLtaS4

and boiled for 20 min. The samples were subsequently centrifuged at 16,000 × *g* for 5 min, and SDS-solubilized LTA was subjected to SDS-PAGE and immunoblotting. Proteins in the second sample were precipitated with 10% trichloroacetic acid for 10 min on ice and sedimented at 16,000 × *g* for 10 min. Protein precipitates were washed with ice-cold acetone, sedimented (16,000 × *g* for 10 min), and air dried. Proteins were suspended in 100 μl of sample buffer with 2% SDS. Aliquots (10 μl) of samples were separated on 15% (vol/vol) polyacrylamide (PAA) gels and electrotransferred to polyvinylidene difluoride (PVDF) membranes. Polyglycerol phosphate was detected with LTA-specific monoclonal antibody (clone 55; HyCult Biotechnology, Uden, The Netherlands) and horseradish peroxidase (HRP)-linked anti-mouse antibodies (Cell Signaling Technology, Danvers, MA) at 1:500 and 1:5,000 dilutions, respectively. LtaS1, LtaS2, LtaS3, LtaS4, ribosomal L6, SrtA, and RpoA protein species were detected by incubation with polyclonal sera raised in rabbits using recombinant proteins purified in *E. coli* as described previously (1). Immunoreactive signals were detected by enhanced chemiluminescence detection.

Cultures of *E. coli* transformants harboring pJK4 without an insert or with either the *ltaS1*, *ltaS2*, *ltaS3*, or *ltaS4* gene were diluted from overnight cultures and grown at 37°C for 16 h in the presence of 1 mM IPTG. Culture aliquots of *E. coli* harboring pJK4-*ltaS1* were also collected after 1.5, 4.5, and 16 h following dilution without addition of IPTG. Cultures were all normalized to an OD_{600} of 5. Five milliliters of normalized culture was collected and bacteria sedimented by centrifugation at 16,000 × *g* for 10 min. Bacteria were lysed by boiling for 20 min in 500 μl of SDS sample buffer containing 2% SDS, and insoluble material was sedimented by centrifugation at 16,000 × *g* for 5 min. Sample aliquots (10 μl) were separated on 15% PAA gels, electrotransferred to PVDF membranes, and used for immunoblotting as described above.

Assessing bacterial growth and sporulation efficiency. Growth of vegetative bacilli was compared between strains by monitoring the density of cultures and determining CFU counts of three independent cultures. Bacilli grown overnight were diluted 100-fold into 30 ml of LB medium and incubated at 37°C with shaking. Culture aliquots were withdrawn at defined time intervals, and OD_{600}s were recorded. Aliquots were serially diluted in 10-fold increments and plated on LB agar for enumeration of CFU following overnight incubation of plates at 37°C. Sporulation was assessed by diluting 10-fold overnight cultures of bacilli grown in BHI into modified G medium (25) followed by incubation at 30°C with shaking. Aliquots of cultures were removed at 24 and 72 h and heated or not for 150 min at 65°C to kill vegetative bacilli. Both nonheated and heated aliquots were serially diluted and plated on solid medium for CFU enumeration. Sporulation efficiency was calculated as follows: (viable spores)/(total CFU) × 100.

Light microscopy. Cells were fixed using 4% buffered formalin and observed. Images were obtained with a charge-coupled-device (CCD) camera on an Olympus IX81 microscope using 100× and 40× objectives. The lengths of bacilli was measured directly from acquired differential interference contrast microscopy (DIC) images using ImageJ and converted to lengths in micrometers using reference images with an objective micrometer. The data were displayed in a box and whisker plot.

Scanning electron microscopy. Bacteria grown on solid medium were suspended in water, washed twice, and fixed for 30 min with 2% glutaraldehyde in phosphate-buffered saline (PBS) at room temperature, and they were then postfixed for 30 min in glutaraldehyde onto freshly prepared poly-L-lysine-coated glass coverslips. Samples were washed twice with PBS and subsequently serially dehydrated by consecutive incubations in 25% and 50% ethanol-PBS, 75% and 90% ethanol-H_2O, and 100% ethanol (twice), followed by 50% ethanol-hexamethyldisilazane

(HDMS) and 100% HDMS. After overnight evaporation of HDMS at room temperature, samples were mounted onto specimen mounts (Ted Pella, Inc., Redding, CA) and coated with 80% Pt–20% Pd to 8 nm using a Cressington 208HR sputter coater at 20 mA prior to examination with a Fei Nova NanoSEM 200 scanning electron microscope (FEI Co., Hillsboro, OR). The scanning electron microscope (SEM) was operated with an acceleration voltage of 5 kV, and samples were viewed at a distance of 5 mm.

Thin sectioning and transmission electron microscopy. Bacteria grown on solid medium were harvested from plates, washed twice in water, and fixed with 2% glutaraldehyde–4% paraformaldehyde in 0.1 M sodium cacodylate buffer (pH 7.2) for 2 h. Fixed cells were washed three times with sodium cacodylate buffer and postfixed for 60 min in sodium cacodylate buffer containing 1% osmium tetroxide. Following these treatments, cells were washed twice with sodium cacodylate buffer and once with 0.04 M maleate buffer (pH 5.1) and subsequently stained for 60 min with 1% uranyl acetate in maleate buffer (pH 6.0). Cells were washed three times with maleate buffer prior to dehydration by successive incubations with 25%, 50%, 70%, 90%, and 100% ethanol and 100% propylene oxide. Cells were infiltrated by two consecutive incubations in 66% propylene oxide–33% Spurr resin and 50% propylene oxide–50% Spurr resin for 30 min, followed by 100% Spurr resin for 6 h, and finally incubated overnight at 60°C. Ninety-nanometer thin sections were cut using a Reichert-Jung (Scotia, NY) Ultracut E microtome and attached to copper grids (200 mesh). Thin sections were subsequently negatively stained using saturated uranyl acetate and lead citrate (Electron Microscopy Services, Hatfield, PA). Images were recorded using a Tecnai F30 (Philips/FEI) transmission electron microscope (field emission gun operating with a 300-kV accelerating voltage, using a magnification of ×15,000 to ×30,000) and a high-performance CCD camera with a resolution of 4,000 by 4,000 pixels. Images were captured using Gatan DigitalMicrograph software and processed using Adobe Photoshop (Adobe, San Jose, CA).

Quantification of cell envelope thickness. The thickness of the cell wall envelope was determined by examining at least 15 thin-sectioned cells observed on micrographs obtained by transmission electron microscopy. Sites along the cell envelope were randomly chosen and the number of pixels (thickness) measured using the measure tool in Adobe Photoshop. The conversion from pixels to thickness (nanometers) was achieved based on the number of pixels corresponding to the length of the scale bar (in nm) of the micrograph. Data were plotted in Graphpad Prism 5.0, and the Student *t* test (unpaired, 2-tailed) was used for statistical analyses.

RESULTS

***ltaS* genes of *B. anthracis*.** A genome search for homologues of the *S. aureus ltaS* gene in *B. anthracis* revealed four genes, BAS2737, BAS5081, BAS3608, and BAS1327, predicted to encode putative sulfatases. The corresponding proteins were found to share 51%, 42%, 41%, and 38% identity with $LtaS_{SA}$, respectively (E values, 0 [BAS2737], 3e−159 [BAS5081], 2e−161 [BAS3608], and 7e−143 [BAS1327]). Sequence alignments and comparisons are provided in Table S1 and Fig. S1 in the supplemental material. The corresponding genes are designated herein *ltaS1* (BAS2737), *ltaS2* (BAS5081), *ltaS3* (BAS3608), and *ltaS4* (BAS1327) and code for predicted products of 657, 642, 639, and 628 amino acids, respectively (Fig. 1A). Several features of *S. aureus* LtaS are conserved in these proteins (Fig. 1A and B). All proteins contain hydrophobic domains predicted to span the plasma membrane five times, with short intervening loops (17). The fifth hydrophobic segment is followed by a predicted signal peptidase I recognition motif (Fig. 1A and B). This processing site has been confirmed for $LtaS_{SA}$ (39, 44), and a similar processing is observed for the LtaS enzymes of *B. anthracis* (see below).

***B. anthracis* mutants with mutations in individual *ltaS* genes.** To examine the function of *ltaS* genes, in-frame deletions in the *ltaS1*, *ltaS2*, or *ltaS3* gene of *B. anthracis* strain Sterne ($pXO1^+$ $pXO2^-$) were generated by allelic replacement using a plasmid with a conditional replication defect (30) (Δ*ltaS1*, Δ*ltaS2*, and Δ*ltaS3* in Table 1). *B. anthracis* Sterne mutants with insertional lesions of the *bursa aurealis* element in *ltaS1*, *ltaS3*, or *ltaS4* were identified in the Sphinx collection of transposon insertion mutants (41) (*ltaS1*::Sp, *ltaS3*::Km, and *ltaS4*::Sp in Table 1). These alleles were crossed back into the *B. anthracis* Sterne parent or Δ*ltaS* mutant strain using bacteriophage CP-51 (15). *B. anthracis* variants with deletions or *bursa aurealis* insertions in single *ltaS* genes were not impaired for bacterial growth, as judged by measuring the optical density of replicating vegetative forms in liquid medium (data not shown). A comparison of bacterial shape and cellular morphology using scanning electron microscopy did not reveal any major difference between vegetative wild-type (WT) and *ltaS* mutant bacilli (Fig. 1C). Subtle differences in cell width or length were not accompanied by defects in cell separation or alteration in envelope thickness or sporulation (see Fig. 4 and 5D). Extracts derived from the vegetative forms of *B. anthracis* Sterne and its *ltaS1*::Sp, Δ*ltaS2*, *ltaS3*::Km, and *ltaS4*::Sp mutants were separated on SDS-PAGE gels, transferred to nitrocellulose membranes, and examined for the presence of LTA using a polyglycerol phosphate-specific monoclonal antibody (16) (Fig. 1D).

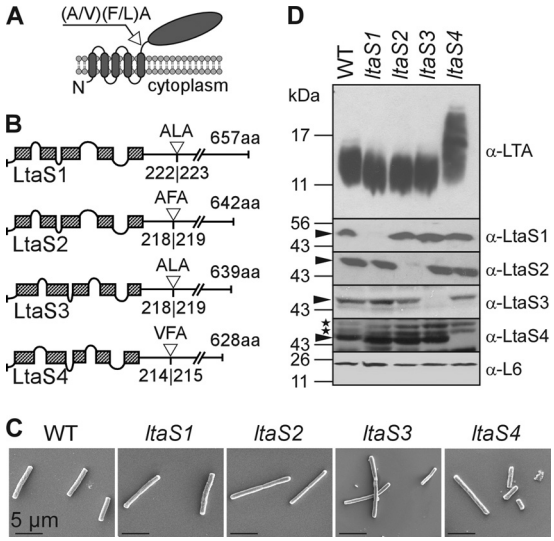

FIG 1 LtaS enzymes of *B. anthracis*. (A) Predicted topology of LtaS homologues in the plasma membrane of *B. anthracis*. LtaS proteins are embedded in the plasma membrane via five predicted transmembrane helices located at the N terminus of the proteins, allowing for extracellular localization of the larger catalytic domain at the C-terminal end of the protein. A single type I signal peptidase cleavage site is found following the last hydrophobic stretch, and signal peptidase cleavage effectively releases the catalytic domain (shown with arrow). (B) Linear models of LtaS enzymes of *B. anthracis* showing the amino acid sequences of predicted cleavage sites (shown with open triangle) and lengths of proteins. The hatched boxes represent hydrophobic regions that span the bilayer. aa, amino acids. (C) Scanning electron microscopy analysis of bacilli (wild type and *ltaS1*, *ltaS2*, *ltaS3*, and *ltaS4* mutants) serially dehydrated and sputter coated with 80% platinum–20% palladium to 8 nm. Scale bar, 50 μm. (D) Synthesis of LTA in *B. anthracis*. Shown are immunoblot analyses of bacterial extracts isolated from the WT and *ltaS1*, *ltaS2*, *ltaS4*, and *ltaS4* mutants by using antibodies specific for LTA, LtaS1, LtaS2, LtaS3, LtaS4, and ribosomal protein L6 (L6, loading control). The migration of protein size standards on SDS-PAGE gels is indicated in kilodaltons. Arrowheads point to processed LtaS proteins, and stars depict the positions of nonspecific cross-reactive immune species.

Extracts from *ltaS1*, *ltaS2*, and *ltaS3* mutants harbored LTA molecules with abundances and mobilities on SDS-PAGE similar to those of the *B. anthracis* Sterne parent strain (Fig. 1D). Extracts of the *ltaS4* mutant also harbored significant amounts of LTA; however, its polyglycerol phosphate molecules migrated with slower mobility and greater heterogeneity than the LTA of *B. anthracis* Sterne (Fig. 1D).

To determine whether LtaS enzymes are expressed in vegetative forms of wild-type and mutant bacilli, we used PCR amplification to clone the coding sequences for the enzymatic domains of LtaS1, LtaS2, LtaS3, and LtaS4 into expression vectors. Thus, only the coding sequences following the predicted signal peptidase I recognition motif as shown on Fig. 1B were included in these clones. His-tagged proteins were purified by affinity chromatography for antibody production in rabbits. Antisera were used for immunoblotting experiments to detect LtaS enzymes in extracts of vegetative forms derived from *B. anthracis* wild-type and *ltaS* mutants (Fig. 1D). The extracts of *B. anthracis* Sterne vegetative forms harbored immunoreactive signals for each of the four enzymes LtaS1 to -4 (Fig. 1D). The electrophoretic mobilities of the four immunoreactive species on 10% SDS-PAGE were consistent with an observed molecular mass of approximately 50 kDa for each one of the four enzymes (Fig. 1D), in agreement with the calculated mass of the signal peptidase cleavage products corresponding to 49,452 Da (LtaS1), 48,749 Da (LtaS2), 48,674 Da (LtaS3), and 473,73 Da (LtaS4). Without processing, the proteins would otherwise display molecular masses of 74,634, 73,469, 73,406, and 72,227 Da, respectively (Fig. 1D). Each of the four *ltaS1* to *-4* mutant strains lacked an immunoreactive signal for the corresponding LtaS enzyme (Fig. 1D). Of note, deletion or insertion mutations in individual *ltaS* genes did not impact the abundance of the remaining three LtaS enzymes (Fig. 1D). As a control, similar intensities of immunoreactive signals for ribosomal protein L6 were detected in the extracts of wild-type and mutant *B. anthracis* strains (Fig. 1D).

LTA synthesis is abrogated in *ltaS1 ltaS2* mutant *B. anthracis*. To test whether LtaS enzymes in *B. anthracis* fulfill redundant functions, we generated variants lacking any two of the four *ltaS* genes (Fig. 2A). Extracts of vegetative forms that had been derived from the isolated mutants were subjected to immunoblotting, which revealed that the *ltaS1 ltaS2* mutant, but not the *ltaS1 ltaS3*, *ltaS1 ltaS4*, *ltaS2 ltaS3*, *ltaS2 ltaS4*, or *ltaS3 ltaS4* variant, was defective for LTA synthesis (Fig. 2A). Of note, the electrophoretic mobility of the LTA of the *ltaS1 ltaS3* and *ltaS2 ltaS3* variants was similar to that of the *B. anthracis* Sterne parent (Fig. 2A). LTA molecules of *ltaS1 ltaS4*, *ltaS2 ltaS4*, and *ltaS3 ltaS4* variants migrated more slowly than and at a speed similar to that of the LTA of the *ltaS4* mutant (Fig. 2A). Further, a strain lacking three *ltaS* genes—*ltaS1*, *ltaS3*, and *ltaS4*—produced LTA with the same electrophoretic mobility as that of the *ltaS4* mutant (Table 1 and Fig. 2A). Repeated attempts to isolate a *B. anthracis* mutant lacking all four *ltaS* genes failed. The LTA synthesis defect of the *ltaS1 ltaS2* mutant was restored following transformation with p*ltaS2*, a plasmid expressing the *ltaS2* gene, but not by the pJK4 vector plasmid (Fig. 2B). The growth of *B. anthracis* vegetative forms in laboratory media was not impaired in strains harboring *ltaS1 ltaS3*, *ltaS1 ltaS4*, *ltaS2 ltaS3*, *ltaS2 ltaS4*, *ltaS3 ltaS4*, or *ltaS1 ltaS3 ltaS4* mutations (Fig. 2C). In contrast, mutants lacking the *ltaS1* and *ltaS2* genes displayed a significant defect in growth. The growth defect of *ltaS1 ltaS2* mutants is due to the generation of daughter cells

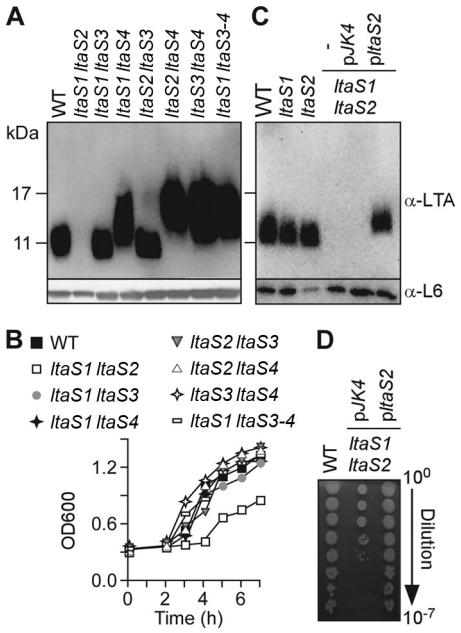

FIG 2 *B. anthracis ltaS1* and *ltaS2* are required for LTA synthesis and bacterial growth. (A) Immunoblot analyses of bacterial extracts isolated from the WT, the *ltaS1 ltaS2*, *ltaS1 ltaS3*, *ltaS1 ltaS4*, *ltaS2 ltaS3*, *ltaS2 ltaS4*, and *ltaS3 ltaS4* double mutants, and the *ltaS1 ltaS3 ltaS4* triple mutant by using antibodies specific for LTA, and ribosomal protein L6 (L6, loading control). The migration of protein size standards on SDS/PAGE gels is indicated in kilodaltons. (B) Growth curves of bacterial strains shown in panel A. Bacteria were diluted in BHI and grown at 37°C with shaking. Bacterial growth was monitored by optical density measurements of cultures at 600 nm (OD_{600}). (C) Expression of *ltaS2* on a plasmid restores LTA synthesis in the *ltaS1 ltaS2* double mutant. Immunoblot analyses were performed as for panel A to compare LTA production among the WT, the *ltaS1* or *ltaS2* mutant, and the *ltaS1 ltaS2* double mutant carrying no plasmid (minus), the plasmid with no insert (pJK4), or the plasmid carrying *ltaS2* (p*ltaS2*). (D) Expression of *ltaS2* on a plasmid restores growth of the *ltaS1 ltaS2* mutant. Bacterial growth was examined by plating serial dilutions (0- to 7-fold) for the WT, *ltaS1 ltaS2* pJK4, and *ltaS1 ltaS2* p*ltaS2*.

that are nonviable, as the plating of aliquots from mutant cultures produced 1,000-fold-fewer colonies on agar media than the plating of aliquots of *B. anthracis* Sterne cultures with equal OD_{600}s (Fig. 2D). The defect in bacterial growth and the generation of viable daughter cells were restored to wild-type levels in the *ltaS1 ltaS2* mutant harboring p*ltaS2* but not by the *ltaS1 ltaS2* mutant with pJK4 vector control (Fig. 2D). Overproduction of LtaS1 from the pJK4 plasmid was poorly tolerated in all species (including *E. coli* and *S. aureus*), and thus, the complementation studies were performed with the pJK4-*ltaS2* (p*ltaS2*) plasmid exclusively.

LTA synthesis promoted by *B. anthracis* LtaS enzymes in heterologous hosts. Expression of *S. aureus ltaS* from a plasmid with an inducible promoter in *E. coli* leads to the synthesis of polyglycerol phosphate LTA from phosphatidylglycerol (17). To test whether each of the four LtaS enzymes of *B. anthracis* is sufficient to promote synthesis of LTA, each gene was expressed from a plasmid in *E. coli* (Fig. 3A to C). Production of all the enzymes was observed upon addition of an inducer (IPTG) at mid-logarithmic growth; of note, LtaS4 was produced in moderate amounts compared to LtaS1, LtaS2, and LtaS3 (Fig. 3B). Immunoblotting experiments with bacterial extracts revealed the presence of polyglycerol phosphate in cells harboring p*ltaS2* and

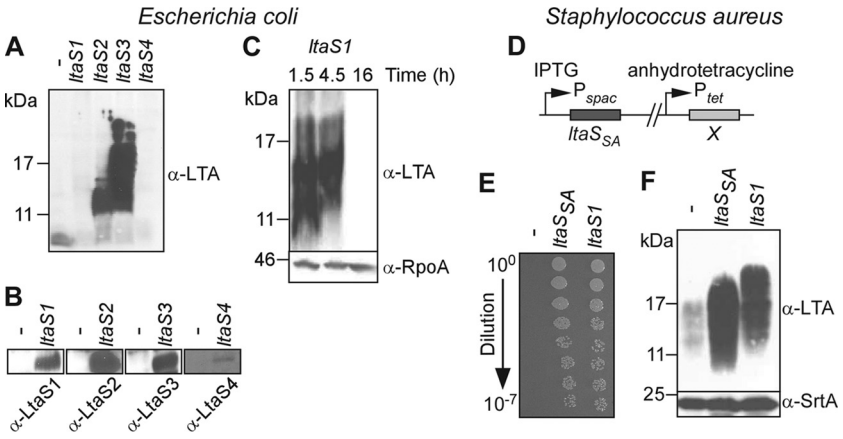

FIG 3 *B. anthracis* LtaS1, LtaS2, and LtaS3 catalyze LTA synthesis in heterologous hosts. (A to C) Expression of *B. anthracis* LtaS1, LtaS2, and LtaS3 in *E. coli* promotes synthesis of polyglycerol phosphate. *E. coli* strains carrying pJK4 with no insert (minus) or with an insert (*ltaS1*, *ltaS2*, *ltaS3*, and *ltaS4*) were grown for 16 h in the presence of IPTG (A and B), and *E. coli* pJK4-*ltaS1* was grown for 1.5, 4.5, and 16 h in the absence of IPTG (C). Extracts from normalized culture aliquots were separated by SDS-PAGE for immunoblot detection of LTA (A to C), LtaS enzymes, and RpoA (loading control) using specific antibodies (B). (D to F) Functional complementation of *ltaS* depletion in *S. aureus* with *B. anthracis ltaS1* homologue. (D) Schematic representation of chromosomal organization in *ltaS* complementation strains. *S. aureus* cultures of strains carrying either no insert (minus), *S. aureus* $ltaS_{SA}$, or *B. anthracis ltaS1* at position X were grown overnight in the presence of IPTG. The following day, cultures were washed and diluted in fresh medium containing anhydrotetracycline only and analyzed for restoration of staphylococcal growth (E) as described for Fig. 2D and LTA production (F) by using antibodies specific for LTA and sortase A (SrtA; loading control). The values to the left of panels A, C, and F indicate the migration of protein size standards, in kilodaltons.

p*ltaS3* but not in vector control cells (Fig. 3A). LtaS4-mediated production of polyglycerol phosphate was never observed regardless of the medium or density of the cell culture. Expression of *ltaS1* was poorly tolerated in *E. coli*, and polyglycerol phosphate production could be observed only in cultures grown in the absence of an inducer (IPTG) to mid-logarithmic growth (Fig. 3C). To analyze the function of *ltaS1* further, we used an *S. aureus* mutant in which the *ltaS* gene was placed under the control of the IPTG-inducible P_{spac} promoter (17) and the *B. anthracis ltaS1* gene was cloned under the control of the anhydrotetracycline-inducible P_{tet} promoter in the chromosome (Fig. 3D). When grown at 37°C in the presence of anhydrotetracycline (and in the absence of IPTG), *S. aureus* expressing *B. anthracis ltaS1* formed colonies on TSB agar (Fig. 3E). As a control, the staphylococcal mutant without an insertion of *ltaS* at the P_{tet} promoter did not form colonies (Fig. 3E). This result is in agreement with earlier findings that LTA synthesis is essential for *S. aureus* growth at 37°C (17). A variant harboring the staphylococcal $ltaS_{SA}$ gene under the control of P_{tet} generated similar numbers of viable colonies as the mutant expressing *B. anthracis ltaS1* (Fig. 3E). Staphylococcal extracts were subjected to immunoblotting with monoclonal antibody specific for polyglycerol phosphate. *S. aureus* P_{spac}-*ltaS* mutant cultures diluted into medium without the inducer IPTG produced only small amounts of immunoreactive LTA. This defect in LTA synthesis was alleviated when P_{spac}-*ltaS* mutants harbored a chromosomal insertion of P_{tet}-$ltaS_{SA}$ or of P_{tet}-*ltaS1* (Fig. 3F). These two strains produced similar amounts of immunoreactive LTA; however, the polyglycerol phosphate of the P_{tet}-*ltaS1* mutant strain migrated more slowly on SDS-PAGE than that of P_{tet}-$ltaS_{SA}$ mutant staphylococci, suggesting that the *B. anthracis* LtaS1 enzyme may generate LTA molecules with increased chain length compared to that of the LTA molecules produced by staphylococcal LtaS (Fig. 3F). Taken together, the results in Fig. 3 indicate that *B. anthracis ltaS1* and *ltaS2* encode polyglycerol phosphate synthases with redundant or partially overlapping functions, which may explain why each of the two genes can be deleted without affecting *B. anthracis* growth.

Microscopic visualization of wild-type and *ltaS* mutant *B. anthracis* Sterne. Vegetative forms of *B. anthracis* Sterne and the four *ltaS* mutants (*ltaS1* to *-4*) were subjected to scanning electron microscopy. Both wild-type and *ltaS* mutant strains appeared as rod-shaped cells or short chains, and they did not display major differences in their cell morphology (Fig. 1D). In contrast, cells of the *ltaS1 ltaS2* double mutant appeared as filamentous chains. To measure the chain length of bacilli, strains were grown on plates and isolated colonies were suspended in liquid medium and analyzed by light microscopy (Fig. 4; 100 chains were measured for each strain). *B. anthracis* Sterne formed chains that were, on average, 9.86 (±0.66) μm in length. Chains of each single mutant displayed similar lengths, with perhaps the exception of the *ltaS3*

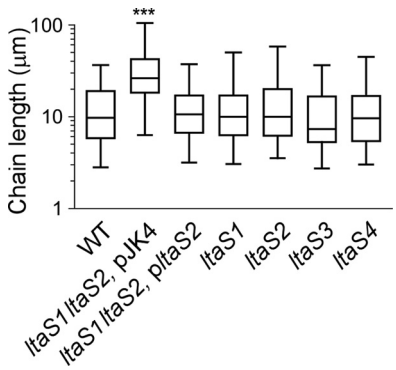

FIG 4 Box and whisker plot of the chain lengths of *B. anthracis* Sterne (WT) and variants with mutational lesions in *ltaS1* and *ltaS2* harboring or not p*ltaS2*, as well as *ltaS1*, *ltaS2*, *ltaS3*, or *ltaS4*, grown on LB agar. Chain lengths were measured from DIC micrographs of vegetative bacilli ($n = 100$; micrographs not shown). ***, statistical significance was established with the unpaired, two-tailed Student *t* test ($P < 0.001$).

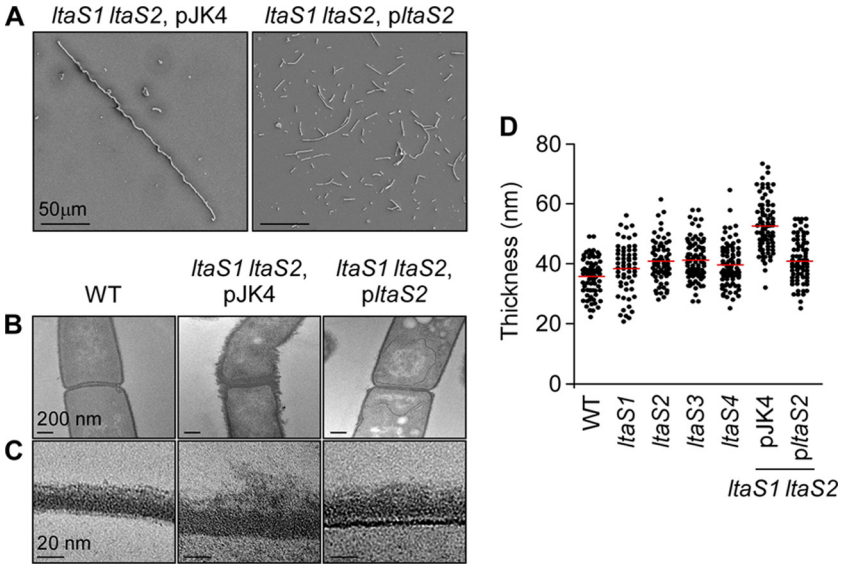

FIG 5 Electron microscopy analysis of vegetative bacilli. (A) Scanning electron microscopy analysis of bacilli (WT, *ltaS1 ltaS2* pJK4 [double mutant carrying the empty vector], and *ltaS1 ltaS2* p*ltaS2* [complemented strain]) serially dehydrated and sputter coated with 80% platinum–20% palladium to 8 nm. Cells of wild-type and complemented mutant strains appear as rod-shaped bacilli, whereas the *ltaS1 ltaS2* mutant bacilli remain tethered in long chains. Scale bar, 50 μm. (B) Thin-section transmission electron microscopy of the same cells as in panel A showing the irregular and deformed structure of the *ltaS1 ltaS2* mutant compared to that of the WT and complemented strains. Scale bar, 200 nm. (C) Close-up of the cell envelope of thin-sectioned bacilli shown in panel B. The layers, from bottom to top, represent cytoplasm, membrane (thin darker line), envelope, and environmental milieu. Scale bar, 20 nm. (D) Measurement of the thickness of the cell envelope of bacilli. Measurements were performed using transmission electron micrographs as shown in panels B and C. Each dot represents one measurement.

mutant, which seemed to display slightly shorter chains. Yet this difference did not reach statistical significance. The average chain length of the *ltaS1 ltaS2* mutant with empty vector was increased to 24.69 (±1.51) μm (WT versus *ltaS1 ltaS2* mutant, $P < 0.0001$). The presence of pJK4 was not responsible for the increased chain length (data not shown). The chain length phenotype of the *ltaS1 ltaS2* mutant was reduced when *ltaS1 ltaS2* bacilli were transformed with plasmid p*ltaS2* carrying wild-type *ltaS2* (12.43 [±0.691] μm; WT versus *ltaS1 ltaS2* p*ltaS2* mutant, $P < 0.001$). Of note, compared to *B. anthracis* Sterne, the dimensions of individual cells from the *ltaS1 ltaS2* mutant were not altered. This increase in chain length was also observed by scanning electron microscopy (Fig. 5A).

Transmission electron microscopy of thin-sectioned vegetative forms was used to visualize the envelope of *B. anthracis* wild type and *ltaS1 ltaS2* pJK4 and *ltaS1 ltaS2* p*ltaS2* mutant cells (Fig. 5B and C). Images of the envelope of *B. anthracis* Sterne revealed a compact, layered appearance with an average diameter of 35.7 (±0.7) nm ($n = 72$) (Fig. 5D). The envelope of the *ltaS1* mutant displayed comparable morphology, although its diameter was slightly increased (38.4 [±1.1] nm, $n = 61$; WT versus *ltaS1* mutant, $P = 0.035$) (Fig. 5D). The envelope of the *ltaS2* mutant appeared somewhat disordered, and its diameter was also increased (40.9 [±0.8] nm, $n = 71$; WT versus *ltaS2* mutant, $P < 0.001$) (Fig. 5D). Finally, images of the envelope of the *ltaS1 ltaS2* mutant revealed a general disorder in the otherwise organized structure of the *B. anthracis* envelope comprised of peptidoglycan layer, attached secondary cell wall polysaccharide, and S-layer (13, 31) (Fig. 5C). The diameter of the *ltaS1 ltaS2* mutant envelope was determined to be 49.3 (±1.0) nm ($n = 71$), significantly increased in comparison with that of the wild-type or *ltaS1* or *ltaS2* mutant strain ($P < 0.001$; Fig. 5D). We investigated whether the *ltaS1* and *ltaS2* mutations affect the retention of S-layer proteins Sap and EA1 in the bacterial envelope, but we observed no difference with S-layer protein retention compared to that with the wild-type parent strain (data not shown).

LTA synthesis is required for *B. anthracis* sporulation. When nutrients are limiting, *B. anthracis* vegetative cells differentiate into spores, a dormant structure carrying the genetic material of the bacterium (27). The transition from vegetative cells to spores is a series of morphological events that require major remodeling of this microbe's envelope (6). We wondered whether the *ltaS* genes might contribute to sporulation. *B. anthracis* Sterne, wild type and *ltaS* mutants, was grown in modified G medium at 30°C to trigger sporulation. The efficacy of spore formation was assessed by plating culture aliquots for colony formation with and without prior treatment at 65°C, a condition that kills vegetative bacilli but not spores. The efficiency of spore formation was calculated as the ratio of viable spores (heat-resistant CFU) to the total CFU count (no heat treatment) at 24 and 72 h following incubation in modified G medium. The data revealed that the *ltaS1 ltaS2* mutant was unable to form heat-resistant spores, whereas mutants with defects in single genes (*ltaS1*, *ltaS2*, *ltaS3*, and *ltaS4*) did not display a defect (Fig. 6A).

To further characterize the defect in sporulation of the *ltaS1 ltaS2* mutant, aliquots of *B. anthracis* cultures were subjected to transmission electron microscopy (Fig. 6B). Forty hours after the dilution of vegetative forms into G medium, *B. anthracis* Sterne cultures harbored only endospores. At the same time point and at 136 h, the *ltaS1 ltaS2* mutant cultures harbored elongated vegetative bacilli but no spores. This defect was partially overcome when the *ltaS1 ltaS2* mutant carried p*ltaS2*, although the formation of

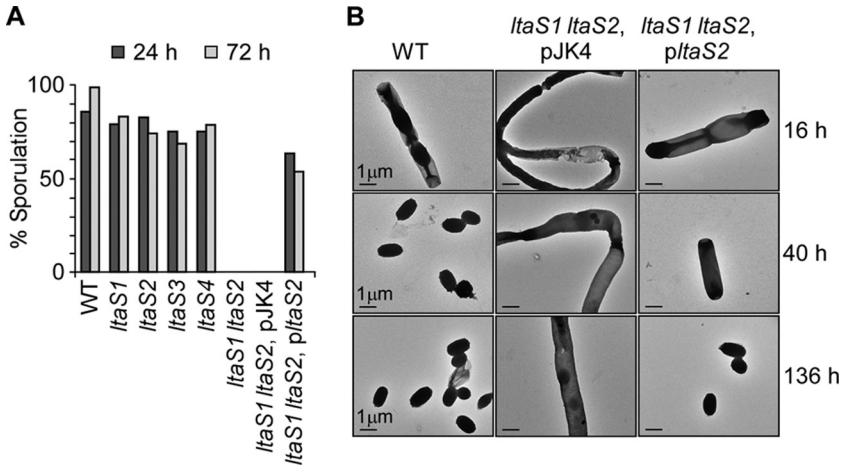

FIG 6 LtaS1 and LtaS2 are required for spore formation. (A) Sporulation efficiency of wild-type and mutant strains grown in modified G medium for 24 or 72 h and reported as percentage of heat-resistant organisms over total organisms (non-heat treated). Aliquots of cultures were removed at the indicated times, treated or not at 65°C, and plated on solid medium for enumeration of CFU. (B) Spore formation visualized by transmission electron microscopy following 16, 40, and 136 h of incubation of bacteria in modified G medium (WT, *ltaS1 ltaS2* pJK4 [double mutant carrying the empty vector], and *ltaS1 ltaS2* p*ltaS2* [complemented strain]).

spores was significantly delayed (Fig. 6B). In agreement with this result, the efficiency of spore formation in the *ltaS1 ltaS2* (p*ltaS2*) mutant strain was reduced to 63% and, in contrast to that of the wild type, did not increase over time (Fig. 6A). These data indicate that LTA synthesis of *B. anthracis* Sterne is absolutely required for spore formation.

DISCUSSION

LTA synthesis can be divided into the assembly of the glycolipid anchor, the polymerization of polyglycerol phosphate, and the decoration of LTA glycerol 2′OH with D-alanyl esters or *N*-acetylglucosamine (33, 38). In *S. aureus*, the membrane anchor moiety for LTA is composed of β-gentiobiosyldiacylglycerol [glucosyl-(1→6)-glucosyl-(1→3)-diacylglycerol (Glc_2-DAG)] (7). Three enzymes—PgcA (α-phosphoglucomutase), GtaB (UTP:α-glucose-1-phosphate uridyl transferase), and YpfP (glycosyltransferase)—are required to produce Glc_2-DAG (16, 20, 26). LtaA is required for moving Glc_2-DAG across the membrane (16). Finally, LtaS polymerizes phosphatidylglycerol into polyglycerol phosphate while generating DAG as a secondary product (17).

The genome of *B. anthracis* contains homologues of *pgcA* (BAS4790), *gtaB* (BAS4789), and *ypfP* (BAS0483), but not *ltaA*. LtaA is a member of the major facilitator superfamily of proteins, of which *B. anthracis* encodes several different members (28). Interestingly, the glycolipid anchor of *B. subtilis* LTA assumes the same chemical structure as the membrane anchor of *S. aureus* LTA (5, 7). With the notable exception of *ltaA*, *B. subtilis* uses the same enzymes as described for the synthesis of the *S. aureus* glycolipid (21, 38). Similar to that of *B. anthracis*, the genome of *B. subtilis* encodes four LtaS homologues (17). Mutants lacking one of these genes, *yflE* ($ltaS_{BS}$), grow more slowly than the wild type and display a defect in divalent cation homeostasis, an increase in chain length, and placement of aberrant septa, as well as enhanced cell bending and lysis (40). YflE ($LtaS_{BS}$) has been referred to as the housekeeping synthase (40, 43). A mutant lacking all four paralogues of *ltaS* remains viable, albeit with severe morphological defects in cell structure and with elongated filaments of *B. subtilis* vegetative forms (40, 43). *In vitro* and *in vivo* biochemical analyses revealed that all four LtaS paralogues are active in cleaving phosphatidylglycerol to generate DAG. Three enzymes—YflE ($LtaS_{BS}$), YfnI, and YqgS—generate polyglycerol phosphate in *B. subtilis* and in *S. aureus* (43). YfnI generates high-molecular-weight polyglycerol phosphate polymers, but their function is unknown (43). The fourth enzyme, YvgJ, adds a single glycerol phosphate moiety to Glc_2-DAG, which earned the enzyme the designation LTA primase (42, 43). Of note, LTA primase expression is not required for the synthesis of glycolipid-linked LTA in either *B. subtilis* or *L. monocytogenes* (42, 43). Although the product of the LTA primase reaction is thought to be a precursor for LTA synthesis, it is also conceivable that the primase product is not a substrate for LTA synthesis and instead fulfills another function. Furthermore, there appear to be differences in the structures of the LTA products derived from YflE ($LtaS_{BS}$), YfnI, and YqgS (43). YflE ($LtaS_{BS}$) and YfnI generated significant amounts of LTA in *S. aureus*, yet only *yflE* ($ltaS_{BS}$), not *yfnI*, supported the growth of *ltaS*-deficient *S. aureus* (17). *B. subtilis* mutants lacking $ltaS_{BS}$ and *yfnI*, but not mutants with mutations in single *ltaS* genes, are defective for LTA synthesis.

Here we report for the first time that *B. anthracis* synthesizes polyglycerol phosphate LTA molecules. Our findings are in disagreement with earlier work reporting that glycerol phosphate polymers are absent from the envelope of *B. anthracis* (32). The genome of *B. anthracis* harbors four homologues of *S. aureus* LtaS, and two of these, LtaS1 and LtaS2, are sufficient to synthesize polyglycerol phosphate LTA in *B. anthracis* and in heterologous hosts, *S. aureus* or *E. coli*. It is conceivable that one or both of the other two LtaS enzymes (LtaS3 and LtaS4) act as LTA primases (42). Alternatively, these enzymes may synthesize small amounts of LTA at unique stages or locations during the *B. anthracis* life cycle. We noted that *ltaS1 ltaS2* mutants are defective in sporulation and vegetative growth. It seems plausible to us that LTA synthesis of *B. anthracis* is essential for the growth of this microbe under physiological conditions. If so, LtaS enzymes would represent a valuable target for the devel-

opment of antibiotic compounds that can be used for the treatment and prevention of biodefense and emerging infectious disease threats (36). Considering the presence of the *pgcA*, *gtaB*, and *ypfP* genes in the chromosome of *B. anthracis*, we think it is likely that this organism also synthesizes Glc_2-DAG membrane anchors for its LTA molecules. Our discovery of LTA in the envelope of *B. anthracis* suggests further that the physiological role of the microbe's *dltABCD* operon is likely the D-alanyl esterification of polyglycerol phosphates (12). Future work must address the chemical nature of the presumed glycolipid anchor and alanyl esterification of polyglycerol phosphates by purifying LTA molecules from the envelope of *B. anthracis* and determining their chemical structure.

It is intriguing that the phenotypic defects associated with specific *ltaS* mutants do not point to specific sequence features of the corresponding enzymes. LtaS homologues of *B. anthracis*, *B. subtilis*, and *S. aureus* share 38 to 78% identity at the amino acid level throughout their sequences (Table S1; Fig. S1). *B. anthracis* LtaS1 is most homologous to the housekeeping LTA synthase YflE ($LtaS_{BS}$) and YfnI (the enzyme that produces large LTA polymers). LtaS2, LtaS3, and LtaS4 share the highest homology with YqgS (the enzyme involved in sporulation). Overall, LtaS2 and LtaS3 share the greatest amino acid sequence identity, 78%, yet the *ltaS1 ltaS3* double mutant behaved mostly like the wild type, unlike the *ltaS1 ltaS2* double mutant (Table S1; Fig. S1). In *B. anthracis*, LtaS1 and LtaS2 represent the housekeeping synthases. Defects in cell separation, growth, and sporulation are associated with failure to produce LTA in the *ltaS1 ltaS2* double mutant. Similar phenotypic defects do not directly correlate with loss of LTA synthesis in *B. subtilis*; indeed, mutants displaying cell chaining, growth, and sporulation defects could still synthesize LTA (43). Perhaps this difference can be attributed to the fact that unlike *B. anthracis*, *B. subtilis* produces wall teichoic acid (WTA). An attempt to delete *tagO*, the gene that encodes the enzyme initiating synthesis of WTA in the *yflE yfnI yqgS yvgJ* quadruple mutant, was unsuccessful, suggesting that WTA and LTA may fulfill redundant functions in *B. subtilis* (40).

It has been suggested that round, spherical microbes (cocci) producing LTA—e.g., *Staphylococcus* spp., *Streptococcus* spp., and *Lactococcus lactis*—harbor a single *ltaS* gene. Organisms with more diverse cell shapes, e.g., ellipsoid microbes such as *E. faecalis* as well as rod-shaped *Listeria* spp., carry at least two *ltaS* genes. Finally, rod-shaped bacteria with complex developmental cycles (e.g., spore formation) such as *B. subtilis* encode four LtaS-like proteins. In all cases examined, abolishing LTA production by mutagenesis of cognate *ltaS* genes leads to morphological changes and cell division defects, suggesting that LtaS-mediated synthesis of LTA appears to fulfill a universal function for cell division.

ACKNOWLEDGMENTS

We thank members of the Schneewind and Missiakas laboratories for discussions.

We acknowledge membership within and support from the Region V 'Great Lakes' Regional Center of Excellence in Biodefense and Emerging Infectious Diseases Consortium (GLRCE, NIAID Award 1-U54-AI-057153). J.W.K. acknowledges support from the Molecular Cell Biology Training Grant (GM007183).

REFERENCES

1. **Anderson VJ, Kern JW, McCool JW, Schneewind O, Missiakas D.** 2011. The SLH-domain protein BslO is a determinant of Bacillus anthracis chain length. Mol. Microbiol. **81**:192–205.
2. **Araki Y, Ito E.** 1989. Linkage units in cell walls of Gram-positive bacteria. Crit. Rev. Microbiol. **17**:121–135.
3. **Baddiley J.** 1968. Teichoic acids in walls and the molecular structure of bacterial walls. Proc. R. Soc. Lond. B Biol. Sci. **170**:331–348.
4. **Choudhury B, et al.** 2006. The structure of the major cell wall polysaccharide of *Bacillus anthracis* is species specific. J. Biol. Chem. **281**:27932–27941.
5. **Coley J, Duckworth M, Baddiley J.** 1972. The occurrence of lipoteichoic acids in the membranes of Gram-positive bacteria. J. Gen. Microbiol. **73**:587–591.
6. **Driks A.** 2002. Maximum shields: the assembly and function of the bacterial spore coat. Trends Microbiol. **10**:251–254.
7. **Duckworth M, Archibald AR, Baddiley J.** 1975. Lipoteichoic acid and lipoteichoic acid carrier in *Staphylococcus aureus* H. FEBS Lett. **53**:176–179.
8. **Emdur L, Chiu T-H.** 1975. The role of phosphatidylglycerol in the in vitro biosynthesis of teichoic acid and lipoteichoic acid. FEBS Lett. **55**:216–219.
9. **Fischer B, et al.** 1996. Novel animal model for studying the molecular mechanisms of bacterial adhesion to bone-implanted metallic devices: role of fibronectin in *Staphylococcus aureus* adhesion. J. Orthop. Res. **14**: 914–920.
10. **Fischer W.** 1990. Bacterial phosphoglycolipids and lipoteichoic acids, p 123–234. *In* Hanahan DJ (ed), Handbook of lipid research, vol 6. Plenum Press, New York, NY.
11. **Fischer W, Koch HU, Rösel P, Fiedler F, Schmuck L.** 1980. Structural requirements of lipoteichoic acid carrier for recognition by the poly(ribitol phosphate) polymerase from *Staphylococcus aureus* H: a study of various lipoteichoic acids, derivatives, and related compounds. J. Biol. Chem. **255**:4550–4556.
12. **Fisher N, et al.** 2006. The *dltABCD* operon of *Bacillus anthracis* Sterne is required for virulence and resistance to peptide, enzymatic, and cellular mediators of innate immunity. J. Bacteriol. **188**:1301–1309.
13. **Fouet A.** 2009. The surface of *Bacillus anthracis*. Mol. Aspects Med. **30**: 374–385.
14. **Glaser L, Lindsay B.** 1974. The synthesis of lipoteichoic acid carrier. Biochem. Biophys. Res. Commun. **59**:1131–1136.
15. **Green BD, Battisti L, Koehler TM, Thorne CB, Ivins BE.** 1985. Demonstration of a capsule plasmid in *Bacillus anthracis*. Infect. Immun. **49**: 291–297.
16. **Gründling A, Schneewind O.** 2007. Genes required for glycolipid synthesis and lipoteichoic acid anchoring in *Staphylococcus aureus*. J. Bacteriol. **189**:2521–2530.
17. **Gründling A, Schneewind O.** 2007. Synthesis of glycerol phosphate lipoteichoic acid in *Staphylococcus aureus*. Proc. Nat. Acad. Sci. U. S. A. **104**: 8478–8483.
18. **Heaton MP, Neuhaus FC.** 1992. Biosynthesis of D-alanyl-lipoteichoic acid: cloning, nucleotide sequence, and expression of the *Lactobacillus casei* gene for the D-alanine-activating enzyme. J. Bacteriol. **174**:4707–4717.
19. **Heaton MP, Neuhaus FC.** 1994. Role of the D-alanyl carrier protein in the biosynthesis of D-alanyl-lipoteichoic acid. J. Bacteriol. **176**:681–690.
20. **Jorasch P, Warnecke DC, Lindner B, Zahringer U, Heinz E.** 2000. Novel processive and nonprocessive glycosyltransferases from *Staphylococcus aureus* and *Arabidopsis thaliana* synthesize glycolipids, glycophospholipids, glycosphingolipids, and glycosylsterols. Eur. J. Biochem. **267**:3770–3783.
21. **Jorasch P, Wolter FP, Zahringer U, Heinz E.** 1998. A UDP glucosyltransferase from *Bacillus subtilis* successively transfers up to four glucose residues to 1,2-diacylglycerol: expression of *ypfP* in *Escherichia coli* and structural analysis of its reaction products. Mol. Microbiol. **29**:419–430.
22. **Karatsa-Dodgson M, Wörmann ME, Gründling A.** 2010. *In vitro* analysis of the *Staphylococcus aureus* lipoteichoic acid synthase enzyme using fluorescently labeled lipids. J. Bacteriol. **192**:5341–5349.
23. **Kern J, Ryan C, Faull K, Schneewind O.** 2010. *Bacillus anthracis* surface-layer proteins assemble by binding to the secondary cell wall polysaccharide in a manner that requires *csaB* and *tagO*. J. Mol. Biol. **401**:757–775.
24. **Kern JW, Schneewind O.** 2008. BslA, a pXO1-encoded adhesin of *Bacillus anthracis*. Mol. Microbiol. **68**:504–515.

25. **Kim HU, Goepfert JM.** 1974. A sporulation medium for *Bacillus anthracis*. J. Appl. Bacteriol. **37**:265–267.
26. **Kiriukhin MY, Debabov DV, Shinabarger DL, Neuhaus FC.** 2001. Biosynthesis of the glycolipid anchor in lipoteichoic acid of *Staphylococcus aureus* RN4220: role of YpfP, the diglucosyldiacylglycerol synthase. J. Bacteriol. **183**:3506–3514.
27. **Koch R.** 1876. Die Ätiologie der Milzbrand-Krankheit, begründet auf die Entwicklungsgeschichte des *Bacillus anthracis*. Beitr. Biol. Pflanzen **2**:277–310.
28. **Law CJ, Maloney PC, Wang DN.** 2008. Ins and outs of major facilitator superfamily antiporters. Annu. Rev. Microbiol. **62**:289–305.
29. **Lazarevic V, Karamata D.** 1995. The *tagGH* operon of *Bacillus subtilis* 168 encodes a two-component ABC transporter involved in the metabolism of two wall teichoic acids. Mol. Microbiol. **16**:345–355.
30. **Marraffini LA, Schneewind O.** 2006. Targeting proteins to the cell wall of sporulating *Bacillus anthracis*. Mol. Microbiol. **62**:1402–1417.
31. **Mesnage S, Tosi-Couture E, Gounon P, Mock M, Fouet A.** 1998. The capsule and S-layer: two independent and yet compatible macromolecular structures in *Bacillus anthracis*. J. Bacteriol. **180**:52–58.
32. **Molnár J, Prágai B.** 1971. Attempts to detect the presence of teichoic acid in *Bacillus anthracis*. Acta Microbiol. Acad. Sci. Hung. **18**:105–108.
33. **Neuhaus FC, Baddiley J.** 2003. A continuum of anionic charge: structures and functions of D-alanyl-teichoic acids in gram-positive bacteria. Microbiol. Mol. Biol. Rev. **67**:686–723.
34. **Oku Y, et al.** 2009. Pleiotropic roles of polyglycerolphosphate synthase of lipoteichoic acid in growth of *Staphylococcus aureus* cells. J. Bacteriol. **191**:141–151.
35. **Peschel A, et al.** 1999. Inactivation of the *dlt* operon in *Staphylococcus aureus* confers sensitivity to defensins, protegrins, and other antimicrobial peptides. J. Biol. Chem. **274**:8405–8410.
36. **Peters NK, Dixon DM, Holland SM, Fauci AS.** 2008. The research agenda of the National Institute of Allergy and Infectious Diseases for antimicrobial resistance. J. Infect. Dis. **197**:1087–1093.
37. **Read TD, et al.** 2003. The genome sequence of *Bacillus anthracis* Ames and comparison to closely related bacteria. Nature **423**:81–86.
38. **Reichmann NT, Gründling A.** 2011. Location, synthesis and function of glycolipids and polyglycerolphosphate lipoteichoic acid in Gram-positive bacteria of the phylum Firmicutes. FEMS Microbiol. Lett. **319**:97–105.
39. **Schallenberger MA, Niessen S, Shao C, Fowler BJ, Romesberg FE.** 2012. Type I signal peptidase and protein secretion in Staphylococcus aureus. J. Bacteriol. **194**:2677–2686.
40. **Schirner K, Marles-Wright J, Lewis RJ, Errington J.** 2009. Distinct and essential morphogenetic functions for wall- and lipo-teichoic acids in *Bacillus subtilis*. EMBO J. **28**:830–842.
41. **Tam C, Glass EM, Anderson DM, Missiakas D.** 2006. Transposon mutagenesis of *Bacillus anthracis* strain Sterne using *bursa aurealis*. Plasmid **56**:74–77.
42. **Webb AJ, Karatsa-Dodgson M, Gründling A.** 2009. Two-enzyme systems for glycolipid and polyglycerolphosphate lipoteichoic acid synthesis in *Listeria monocytogenes*. Mol. Microbiol. **74**:299–314.
43. **Wörmann ME, Corrigan RM, Simpson PJ, Matthews SJ, Gründling A.** 2011. Enzymatic activities and functional interdependencies of *Bacillus subtilis* lipoteichoic acid synthesis enzymes. Mol. Microbiol. **79**:566–583.
44. **Wörmann ME, Reichmann NT, Malone CL, Horswill AR, Gründling A.** 2011. Proteolytic cleavage inactivates the *Staphylococcus aureus* lipoteichoic acid synthase. J. Bacteriol. **193**:5279–5291.
45. **Xia G, Peschel A.** 2008. Toward the pathway of *S. aureus* WTA biosynthesis. Chem. Biol. **15**:95–96.
46. **Yokoyama K, Miyashita T, Arakai Y, Ito E.** 1986. Structure and functions of linkage unit intermediates in the biosynthesis of ribitol teichoic acids in *Staphylococcus aureus* H and *Bacillus subtilis* W23. Eur. J. Biochem. **161**:479–489.